

**Urbach tails of amorphous silicon**

D. A. Drabold, Y. Li, B. Cai, and M. Zhang

*Department of Physics and Astronomy, Ohio University, Athens, Ohio 45701, USA*

(Received 20 September 2010; published 20 January 2011)

In earlier work, we showed that exponential (Urbach) band-edge states were localized on connected subnetworks of short bonds for the valence tail and long bonds for the conduction tail for high-quality continuous random network models of amorphous silicon. Here, we study size effects by computing the electronic density of states for a  $10^5$ -atom model of  $\alpha$ -Si proposed by G. T. Barkema and N. Mousseau [*Phys Rev. B* **62**, 4985 (2000)] and show that the model indeed possesses exponential tails, consistent with earlier calculations on a 4096-atom system. Next, we study the structure of the network near the shortest bonds. These bonds consistently create a slightly densified region, and we discuss the strain field associated with these defects. The dynamics of the short-bond clusters is briefly examined next. We show that there are significant fluctuations in the atoms with instantaneous short bonds, even at 300 K, and we compare the electronic density of states and valence edges between models with filaments and without filaments. We close with speculations on how to determine if the connected subnetwork hypothesis is unique in its ability to produce exponential tails.

DOI: [10.1103/PhysRevB.83.045201](https://doi.org/10.1103/PhysRevB.83.045201)

PACS number(s): 71.23.An, 71.55.Jv

**I. INTRODUCTION**

One of the long-standing research programs for amorphous semiconductors is comprehending the linkage of structural features to electronic or optical characteristics of the material. The classic example is the structural origin of the midgap state in  $\alpha$ -Si or  $\alpha$ -Si:H. As recently as the nineties, there has been a lively debate between proponents of the view that three-coordinated  $sp^3$  dangling bonds were the structural origin or the “floating” (fivefold) bonds. The current prevailing view is that the midgap states are due to dangling bonds.<sup>1</sup>

A more subtle but equally important problem is the structural origin of the exponential or Urbach tails in disordered systems,<sup>2</sup> including  $\alpha$ -Si. Diverse models yielding exponential tails have been advanced, as discussed elsewhere.<sup>3</sup> Recently, we have shown that for  $\alpha$ -Si, the structural features giving rise to the tails in the best available models of the material are a subnetwork of connected short bonds (for the valence tail) and long bonds (for the conduction tail).<sup>4–7</sup> We have shown that the short and long bonds are spatially self-correlated: thus, for example, given a short bond in a network, the likelihood that its neighbors possess a short bond is much higher than random. Also, there is little if any cross-correlation (long to short). The clustered short bonds form a characteristic network—a three-dimensional (3D) structure with short bonds surrounding a particularly short bond.<sup>6</sup> Long bonds form “wispy” or filamentary 1D structures, again, with a high degree of connectivity. We have shown that analogous structures account for the band tails in  $\alpha$ -SiO<sub>2</sub> and other systems.<sup>6</sup> For the sake of convenience, we generically dub connected networks of short bonds or long bonds “filaments” in the rest of this paper.

A feature of all high-quality continuous random network models of  $\alpha$ -Si is that they possess the structural correlations described above. The best models of  $\alpha$ -Si are made with the Wooten–Winer–Weaire (WWW) method<sup>8</sup> and to our knowledge are not in significant contradiction with any experiments (structural, vibrational, or optical). To extend our understanding of these points, we investigate the following four topics in this paper: (1) the role of finite size effects: to

date models with up to 10 000 atoms have been explored with tight-binding in 3D, we extend this to 100 000 atom models in this paper and show that a well-made model of this size produces highly exponential tails; (2) the character of the strain field centered on particularly short bonds; (3) the role of thermal disorder: how thermal fluctuation affects the band tails and how the filaments are affected by thermal disorder; (4) we speculate on the question of the necessity vs sufficiency of the filaments for generating the Urbach tail.

Finally, we observe that the tails are not of mere academic interest. In particular, the broad valence tail in  $\alpha$ -Si:H is a particular culprit in reducing the efficiency of  $\alpha$ -Si:H photovoltaic devices by virtue of reduced hole mobility.<sup>9</sup>

**II. CALCULATIONS ON A LARGE SYSTEM**

By carefully exploiting locality of interactions and implementing various clever computational tricks, Mousseau and Barkema<sup>10</sup> have proposed genuinely enormous, but nevertheless high-quality, models of  $\alpha$ -Si, the largest to date being 100 000 atoms. These models are cubic and periodic boundary conditions are applied. To determine whether the Urbach edges are a property of a large system, we compute the density of states for this model. We show that both tails are quite exponential and indeed very close to an earlier calculation<sup>11</sup> on a smaller (4096-atom) model proposed by Djordjevic and coworkers.<sup>12</sup>

In recent years there have been significant advances in obtaining the electronic structure of large systems. While the roots of these approaches extend back at least to Haydock and Heine’s recursion method,<sup>13</sup> conceptual advances in the nineties showed how to compute total energies and forces in a fashion that scales linearly with system size—the so-called order- $N$  methods.<sup>14</sup> For the present topic, we are concerned primarily with the spectral density of states for a single-particle Hamiltonian in a local basis (orthogonal tight-binding) representation.

Within a tight-binding approach, the electronic Hamiltonian matrix  $H$  of a large model of  $\alpha$ -Si is readily computed because

it is extremely sparse (meaning that the overwhelming majority of the matrix elements vanish). Using the Hamiltonian of Kwon *et al.*<sup>15</sup> (with four orbitals per site and a cutoff between the second and third neighbors for Si) we find that about 54 million matrix elements are nonzero, out of 400 000<sup>2</sup> matrix elements in total, so that only about 1 in 2800 entries in the matrix is nonvanishing. As such, one can take advantage of sparse matrix methods formulated to carry out all matrix operations using only the nonzero matrix elements.

The principle of maximum entropy (maxent) provides a successful recipe for solving missing information problems associated with spectral densities, such as the electronic (or vibrational) density of states.<sup>16</sup> Let  $\rho$  be the maximum entropy estimate for this density. The maxent framework prescribes that we maximize the entropy functional:

$$S[\rho] = - \int d\epsilon \rho(\epsilon) \log[\rho(\epsilon)], \quad (1)$$

subject to the condition that  $\rho(\epsilon)$  satisfies all known information about  $\rho$ , and with implied integration limits over the support of  $\rho$ . As discussed elsewhere,<sup>17</sup> it is easy to get accurate estimates of the power moments  $\mu_i = \int_a^b d\epsilon \epsilon^i \rho(\epsilon)$ ,  $i = 1, N$ . By using simple tricks, one can generate hundreds of power moments in seconds for systems with 10<sup>5</sup> or more atoms (this is because the only operations involving  $H$  are of the form matrix applied to vector). Then maximizing Eq. (1) (solving the Euler equation) subject to the moment data leads to

$$\rho(\epsilon) = \exp \left[ \sum_{i=0}^N \Lambda_i \epsilon^i \right]. \quad (2)$$

From a computational point of view, the maxent moment problem is solved by finding the Lagrange multipliers  $\Lambda$  that satisfy the moment conditions. This system of equations presents a dreary nonlinear problem, but by using orthogonal polynomials rather than raw powers and converting the calculation into a convex optimization problem, practical solutions are available for more than 100 moments.<sup>17-19</sup>

In Fig. 1 we reproduce the electronic density of states for the 10<sup>5</sup>-atom model. We carry out the maxent reconstruction for 107 and 150 moments; the results are nearly identical, implying that the density of states is converged with respect to moment information for of order 100 moments. We show the global density of states, including a state-free optical gap. In Fig. 2, we show a blowup of the gap region. By fitting the tails to an exponential  $\exp(-|E - E_t|/E_U)$ , where  $E_t$  indicates the valence or conduction edge, we obtain Urbach energies of  $E_U = 200$  meV for the valence tail and  $E_U = 96$  meV for the conduction edge. Semilog plots of the density of states for tail energies (not reproduced here) exhibit the expected linear behavior. These Urbach decay parameters are very close to earlier calculations on somewhat smaller systems.<sup>11,20</sup> The small spikes near  $-16.0$  eV are “real”: the moment data and maxent technique produce respectable  $\delta$  functions for isolated states with extremal energies.

We have also determined that the exponential edges are not limited to the valence and conduction tails. The “extremal tails” (near  $-15$  and  $+8$  eV) are also highly exponential. The high-energy edge has an Urbach parameter  $E_U = 130$  meV. The low-energy tail is much sharper than the other

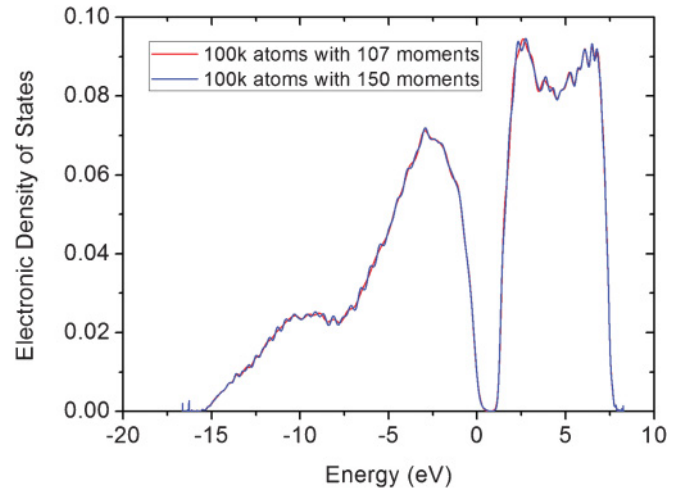


FIG. 1. (Color online) Electronic density of states for 100 000-atom  $\alpha$ -Si model from maxent reconstruction based on 107 and 150 moments. As the curves are nearly identical, ca. 100 moments appears to be sufficient to accurately reproduce the state density. The Fermi level is in the middle of the gap.

three, but still plausibly exponential when plotted on a log scale. It is not possible to access these extremal tails optically or electronically, being so far removed from the Fermi level, yet they do contribute to quantities like the total energy and forces.

We make two additional points. First, the exponential form is in no way due to the maxent approach, which is nonbiased. While the identical calculation has not been published on diamond Si, there are published calculations on very large fullerenes (with up to 3840 atoms, asymptotically approaching graphene) that show a sharp band edge as in crystals, *not* an exponential, an edge that is essentially identical to an exact calculation of the graphene electronic density of states obtained from Brillouin-zone integration.<sup>21</sup> From a mathematical point of view, it is no mean feat for the maxent form [Eq. (2)] to produce simple exponential tails in the gap. In effect, the

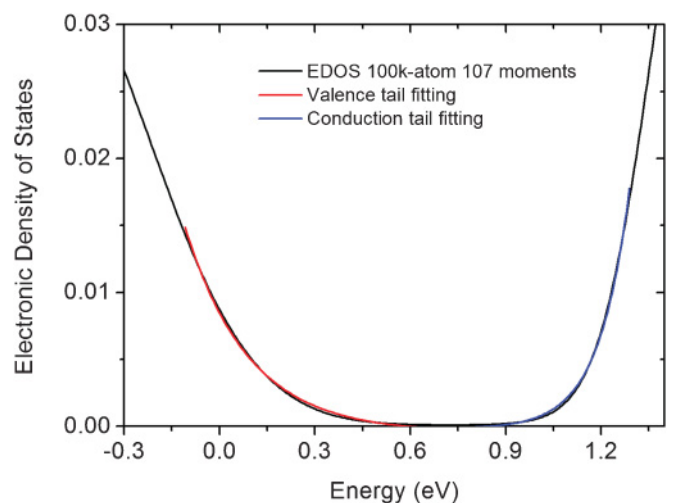


FIG. 2. (Color online) Least-squares fits to exponentials for valence and conduction tails for maxent reconstruction of the density of electron states for 100 000-atom model, based on 107 moments.

network structure of connected filaments (and the consequent electronic Hamiltonian matrix) causes  $\sum_{i=0}^N \Lambda_i \epsilon^i \approx \lambda \epsilon$  for  $\epsilon \in \mathcal{E}$ , where  $\mathcal{E}$  defines a spectral energy range including the two band tails and  $\lambda$  is characteristic of the decay of the valence or conduction tail. Other illustrations can be found in the theory of magnetic resonance.<sup>22</sup> Finally, calculations with more sophisticated (density functional) Hamiltonians (and necessarily smaller models that require Brillouin zone integrations) show exponential tails for topologically similar models.<sup>4,5</sup>

### III. STRAIN RECOVERY FOR SHORT BONDS

We have shown in earlier work that if a particularly short bond appears in the network, it will tend to be connected to other short bonds, which tend to be connected to additional short bonds, etc. Let us name the central short bond a “defect nucleus.” As one progresses away from the nucleus, the bond lengths must asymptotically return to the mean bond length of the network. In effect, there is a strain field induced by the anomalous short bond. In Fig. 3, we illustrate this strain field. There is a reasonably consistent form to the curves, which are plotted for the shortest few bonds in the 512-atom model. By fitting a power law  $\delta r = Ar^\gamma$  (or alternatively, examining a log-log plot), we find that  $\gamma = -1.86 \pm 0.52$ . For several reasons (poor statistics, only a small range of  $r$  contributing meaningful information, etc.) this number is not to be taken too seriously. In fact, we are inclined to wonder if a more refined attempt will not yield a  $1/r$  law, as predicted for a point deformation for a continuum model by Lord Kelvin.<sup>23</sup>

Despite these uncertainties, the consistency of this decay between the different short bond centers is interesting. It seems that to a significant degree, anomalous bonds determine their local topology. Bond length defects have a characteristic spatial range associated with them, and the range is quite predictable for short bond defects, at least. The main point is that one must be careful about thinking in overly local terms—one anomaly affects many atoms. For the case of short bonds, this discussion is salient to the valence tail. In  $\alpha$ -Si, the valence tail is known to be broad and mainly

due to static (not thermal) disorder.<sup>24</sup> In other terms, an individual point defect can introduce density fluctuations on a scale of order  $5\text{--}7\text{\AA}$ .<sup>3</sup> Since short bonds beget short bonds (always with electronic signature at the valence edge), there is a cumulative electronic consequence at the valence edge. Presumably it is this nonlocality and the tendency of the network to local density that makes the valence tail broad (as in an experiment in  $\alpha$ -Si : H in Ref. 9). As we pointed out in the Introduction, for hydrogenated material, the broad valence tail impedes hole mobility. Thus, our calculations suggest that a maximally homogeneous material is ideal for applications. How homogeneous this can be, either in the experimental material or in models is not clear, though we know that the WWW class models are exceptionally uniform compared to models made in other ways.<sup>25</sup>

Where long bonds are concerned, the pattern is less clear because there is a basic asymmetry—sufficiently long bonds are not bonds! Clearly there is no pattern so clear as Fig. 3 for long bonds (since it is silly to imagine that very long, e.g., nonexistent, bonds could induce slightly shorter long bonds, etc.) The experimental observation that the valence tail is much broader than the conduction tail is presumably connected to this basic asymmetry. Bond length distribution is almost symmetric about long and short in a good model. Because the wave functions of the conduction states are mainly distributed in the dilute regions, the disorder potential they feel is weak; thus the conduction tail is less broadened.

### IV. SIZE EFFECTS AND HAMILTONIANS

Because we cannot perform molecular dynamics (MD) simulations on the 100 000-atom model or even the 4096-atom model, we are led to investigate the effects of thermal motion on the filaments and associated electronic structures at the tails. First, we consider the possible importance of size artifacts on the energy spectrum by comparing the 100 000-atom model with a 512-atom model made in a similar way,<sup>12</sup> and we show the result around the gap in Fig. 4. Both plots have similar general features, though the electronic density of states (EDOS) of the 100 000-atom model is of course smoother than

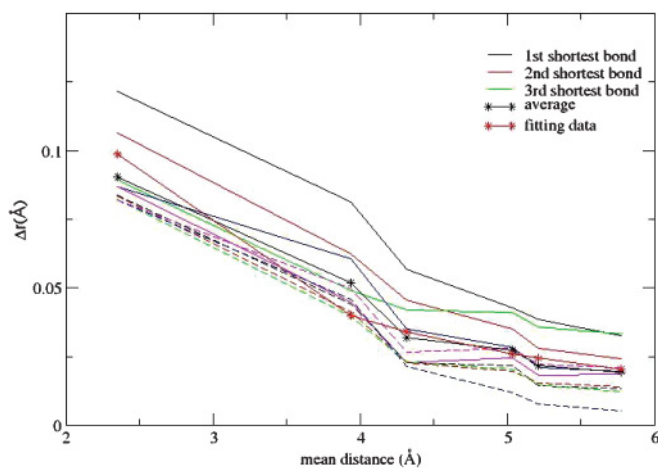


FIG. 3. (Color online) Strain recovery in a 512-atom model of  $\alpha$ -Si: shortest few bonds.  $\Delta r$  is the difference in bond length from the mean;  $r$  is the distance from the short bond defect nucleus.

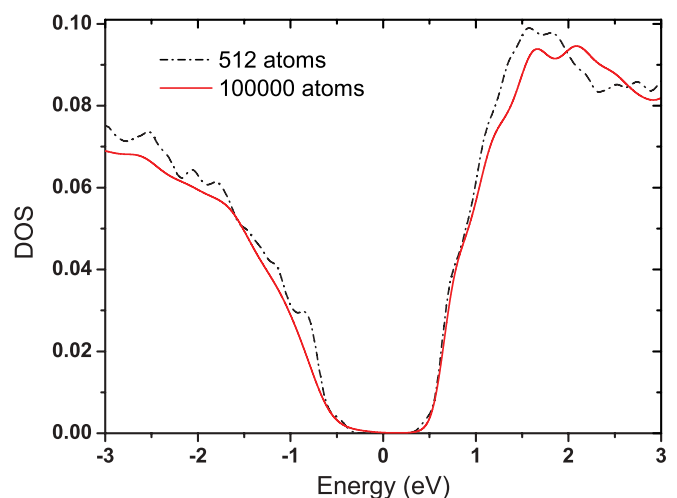


FIG. 4. (Color online) Comparison of electronic density of states between the 512-atom model and the 100 000-atom model.

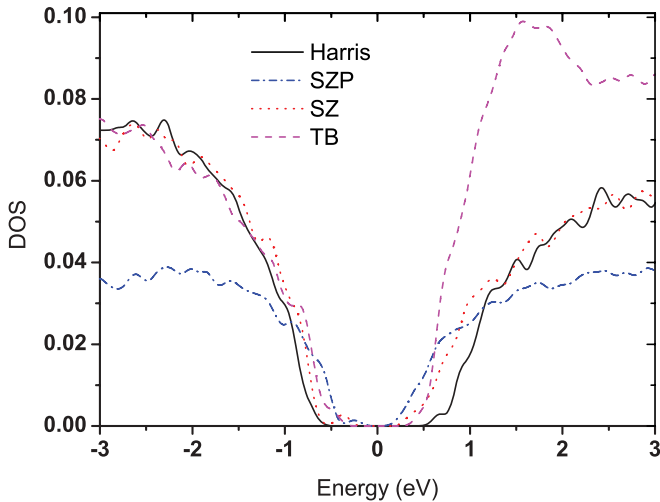


FIG. 5. (Color online) Electronic density of states of 512-atom models obtained by SIESTA self-consistent calculation with single- $\zeta$  and single- $\zeta$ -polarized basis sets, by the tight-binding method, and by a Harris functional calculation with a single- $\zeta$  basis.

that of the 512-atom model. Within finite size artifacts, the 512-atom model is producing a fairly exponential tail which indicates that the 512-atom model is an appropriate basis to study some aspects of the tails in  $\alpha$ -Si.

Next, we compare the EDOS of an  $\alpha$ -Si 512-atom model obtained via different Hamiltonians and plot the results in Fig. 5. The EDOS of a 512-atom model are computed by SIESTA self-consistent calculation with single- $\zeta$  and single- $\zeta$ -polarized basis sets, by the tight-binding method, and by SIESTA using a Harris functional calculation with a single- $\zeta$  basis. We point out that the Harris functional calculation gives a significantly bigger highest occupied molecular orbital (HOMO)-lowest unoccupied molecular orbital (LUMO) gap and, as expected, the more complete the basis the smaller the gap. Though the shapes of EDOS are different for different basis sets, we observe that different basis sets all produce qualitatively exponential tails at least within the finite size effects for the small 512-atom model.

## V. FILAMENT DYNAMICS

Total yield photoelectron spectroscopy measurements have shown interesting behavior in the band tails of  $\alpha$ -Si : H and related materials.<sup>1,24</sup> In the experiments of Aljishi *et al.*<sup>24</sup> it was found that the valence tail was due primarily to structural disorder and that the conduction tail was much more temperature dependent, and thus linked to thermal disorder. MD simulations have been applied to model these effects.<sup>26</sup>

As another step toward understanding the effect of a dynamic lattice on the band tails, we have created animations of the dynamics of the short bonds in the 512-atom cell<sup>12</sup> using the local orbital *ab initio* code SIESTA<sup>27</sup> for temperatures from 20 to 700 K (in each case using constant temperature dynamics). In Figs. 6 and 7 we show instantaneous snapshots of the shortest bonds at two different times at 300 K. As inspection of the animation suggests, there is considerable

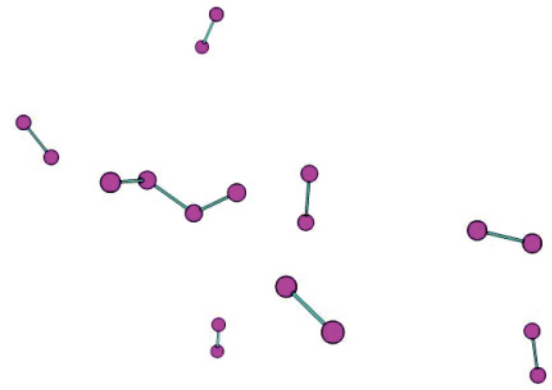


FIG. 6. (Color online) Instantaneous snapshot of short bonds in the 512-atom model at 300 K. Only bonds less than 2.3 Å are shown. A bar connecting the spheres indicates a chemical bond.

fluctuation in the identity of the shortest bonds. While it is not easy to infer from our figures, there is a clear (and expected) tendency for short bonds to occur in the denser volumes near a defect nucleus rather than in other parts of the network. Moreover, we computed the EDOS for a “nonfilament” model and tried to relate it with the Urbach tail. We have also made similar animations for long bonds, and we see extended, highly connected filaments fluctuate into and out of existence. We illustrate the case of short bonds here, as there is less ambiguity in definition. Thus, we note that the filaments persist at room temperature at least,<sup>4</sup> though not by retaining a static form, but with considerable temporal fluctuation. We illustrate these points with animations elsewhere.<sup>28</sup>

We end this section by comparing the EDOS of models with and without filaments. Two 512-atom  $\alpha$ -Si models are presented: one with short and long filaments and the other without filaments.<sup>29</sup> We used the tight-binding method to compute the electronic density of states, and the results are plotted in Fig. 8. A clear band gap exists for the configuration with filaments but a smaller gap is revealed for the model without filaments. Furthermore, we sought to understand the differences

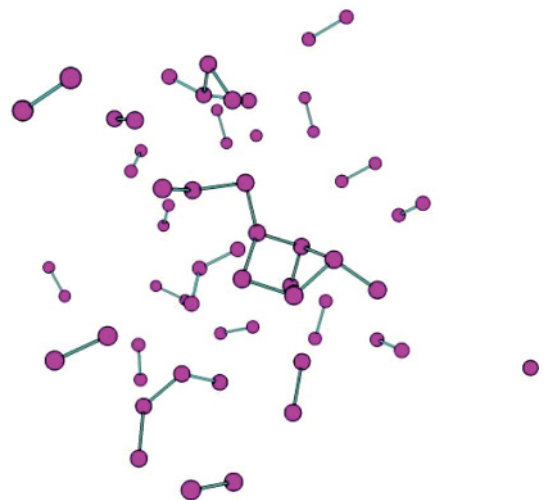


FIG. 7. (Color online) Another instantaneous snapshot of short bonds in a 512-atom model at 300 K. Bonds less than 2.3 Å are shown.

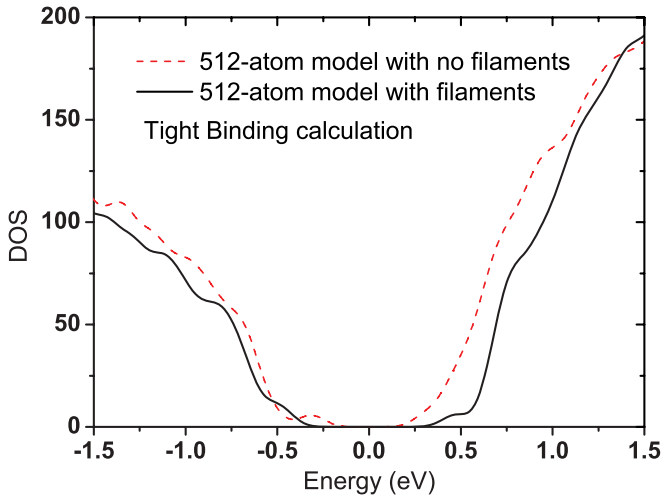


FIG. 8. (Color online) Electronic density of states for 512-atom models with and without filaments.

by performing exponential fits to tails in both models. Because of the incompleteness of the basis set for states above the Fermi level, we only fit the valence tail and we report the outcome in Fig. 9. We found that exponential fits for the structural models with filaments are better than those without filaments. The Urbach energy,  $E_U \approx 193$  meV, is essentially the same as that for the 100 000-atom model for the model including filaments and is  $\approx 99$  meV for the model without filaments. Modification of the filaments leads to significant changes in the Urbach tail.

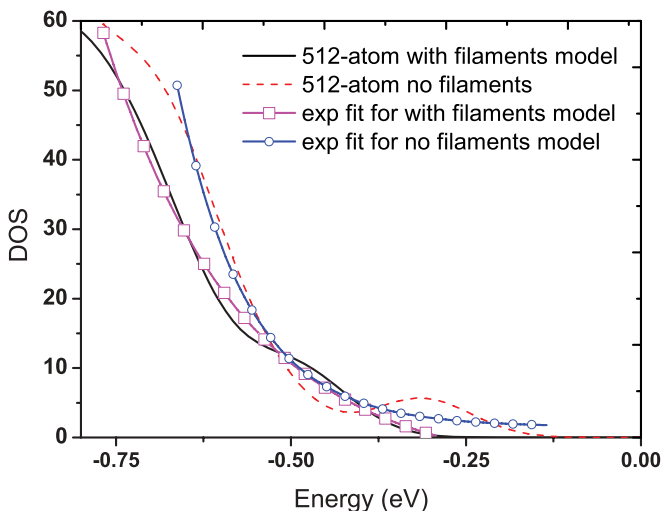


FIG. 9. (Color online) Exponential fitting for valence edges of 512-atom models with and without filaments.

## VI. NECESSITY AND SUFFICIENCY: FILAMENT LOGIC

In this paper and elsewhere,<sup>5</sup> we have shown that filaments  $\Rightarrow$  Urbach edges. But what of necessity: that is, do we know whether Urbach edges  $\Rightarrow$  filaments? The difficulty is that we have to consider how an asymptotically exponential tail constrains the Hamiltonian matrix elements and ultimately what such correlations imply about the topology/connectivity of the  $\alpha$ -Si network in space. We think that it may be useful to approach this with a centrosymmetric single-orbital Hamiltonian. With such a simple beginning, the asymptotic form of the moments is easily computed for exponential tails, and one could then begin to infer the necessary nonrandomness in the Hamiltonian matrix and continue to work backward to models. It is altogether likely that this will not result in a unique structural solution; rather various kinds of configurations probably can lead to exponential tails. A serious constraint must be applied at the end (namely, that the structure must agree with experiments and must be near a local energy minimum for an acceptable interatomic potential, empirical or *ab initio*). Perhaps one concludes with filaments alone at the end of this analysis, but this is uncertain at this point.

An alternative that is perhaps more practical would be to undertake a Monte Carlo simulation with an objective function (or penalty function) which is optimized when a structural model possesses exponential band edges. Atoms might be moved at random to optimize this function according to the conventional Metropolis recipe. If such a stochastic calculation revealed a proclivity for making filaments, necessity might be a reasonable inference.

## VII. CONCLUSION

We have explored some relevant points on the origin of the Urbach tails in  $\alpha$ -Si. The key results are that (1) *all* of the band tails, not just those associated with the optical gap are exponential; (2) very large systems (a  $10^5$ -atom model) possess clearly exponential tails that are highly consistent with smaller models made in a similar way; (3) we find that a power law provides a reasonable fit to the decay of the strain field associated with a short bond defect; and (4) we observe that the filaments persist at finite temperatures, but that they are highly dynamic, even at room temperature.

## ACKNOWLEDGMENTS

We acknowledge the support of the US National Science Foundation under Grant DMR 09-03225 and the Army Research Office under the MURI program (Cooperative Agreement W911NF-0-2-0026). We have benefited from collaboration with F. Inam. We thank Walter Kob for helpful comments on the work. We particularly thank Normand Mousseau and Gerard Barkema for providing their  $10^5$ -atom model of  $\alpha$ -Si.

<sup>1</sup>R. Street, *Hydrogenated Amorphous Silicon* (Cambridge University Press, Cambridge, UK, 1991).

<sup>2</sup>F. Urbach, *Phys. Rev.* **92**, 1324 (1953).

<sup>3</sup>D. A. Drabold, *Eur. Phys. J. B* **68**, 1 (2009).

<sup>4</sup>Y. Pan, M. Zhang, and D. A. Drabold, *J. Non-Cryst. Solids* **354**, 3480 (2008).

<sup>5</sup>Y. Pan, F. Inam, M. Zhang, and D. A. Drabold, *Phys. Rev. Lett.* **100**, 206403 (2008).

- <sup>6</sup>F. Inam, J. P. Lewis, and D. A. Drabold, *Phys. Status Solidi A* **207**, 599 (2010).
- <sup>7</sup>P. A. Fedders, D. A. Drabold, and S. Nakhmanson, *Phys. Rev. B* **58**, 15624 (1998).
- <sup>8</sup>F. Wooten, K. Winer, and D. Weaire, *Phys. Rev. Lett.* **54**, 1392 (1985).
- <sup>9</sup>J. Liang, E. A. Schiff, S. Guha, B. Yan, and J. Yang, *Appl. Phys. Lett.* **88**, 063512 (2006).
- <sup>10</sup>G. T. Barkema and N. Mousseau, *Phys. Rev. B* **62**, 4985 (2000).
- <sup>11</sup>J. Dong and D. A. Drabold, *Phys. Rev. Lett.* **80**, 1928 (1998).
- <sup>12</sup>B. R. Djordjevic, M. F. Thorpe, and F. Wooten, *Phys. Rev. B* **52**, 5685 (1995).
- <sup>13</sup>R. Haydock, in *Solid State Physics*, edited by Henry Ehrenreich, Frederick Seitz, and David Turnbull (Academic Press, New York, 1980), Vol. 35, p. 215.
- <sup>14</sup>P. Ordejon, D. A. Drabold, R. M. Martin, M. P. Grumbach, *Phys. Rev. B* **51**, 1456 (1995).
- <sup>15</sup>I. Kwon, R. Biswas, C. Z. Wang, K. M. Ho, and C. M. Soukoulis, *Phys. Rev. B* **49**, 7242 (1994).
- <sup>16</sup>E. T. Jaynes, *Probability Theory: The Logic of Science* (Cambridge University Press, Cambridge, UK, 2003).
- <sup>17</sup>D. A. Drabold and O. F. Sankey, *Phys. Rev. Lett.* **70**, 3631 (1993).
- <sup>18</sup>L. R. Mead and N. Papanicolaou *J. Math. Phys.* **25**, 2404 (1984).
- <sup>19</sup>K. Bandyopadhyay, A. K. Bhattacharya, P. Biswas, and D. A. Drabold, *Phys. Rev. E* **71**, 057701 (2005).
- <sup>20</sup>J. J. Ludlam, S. N. Taraskin, S. R. Elliott, and D. A. Drabold, *J. Phys. Condens. Matter* **17**, L321 (2005).
- <sup>21</sup>D. A. Drabold, P. Ordejon, J. Dong, and R. M. Martin, *Solid State Commun.* **96**, 833 (1995); R. M. Martin, *Electronic Structure* (Cambridge University Press, Cambridge, UK, 2004), p. 459.
- <sup>22</sup>P. A. Fedders and A. E. Carlsson, *Phys. Rev. B* **32**, 229 (1985); D. A. Drabold and P. A. Fedders, *ibid.* **37**, 3440 (1988).
- <sup>23</sup>L. D. Landau and E. M. Lifshitz, *Theory of Elasticity* (Pergamon, London, 1959), p. 29.
- <sup>24</sup>S. Aljishi, J. D. Cohen, S. Jin, and L. Ley, *Phys. Rev. Lett.* **64**, 2811 (1990).
- <sup>25</sup>M. J. Cliffe, M. T. Dove, D. A. Drabold, and A. L. Goodwin, *Phys. Rev. Lett.* **104**, 125501 (2010).
- <sup>26</sup>D. A. Drabold, P. A. Fedders, S. Klemm, and O. F. Sankey, *Phys. Rev. Lett.* **67**, 2179 (1991).
- <sup>27</sup>E. Artacho, E. Anglada, O. Diéguez, J. D. Gale, A. García, J. Junquera, R. M. Martin, P. Ordejon, J. M. Pruneda, D. Sánchez-Portal, and J. M. Soler, *J. Phys.: Condens. Matter* **20**, 064208 (2008).
- <sup>28</sup>Yuting Li and D. A. Drabold (unpublished).
- <sup>29</sup>The “filament free” model was obtained by performing extended thermal MD simulations at  $T = 300$  K and waiting for an instantaneous conformation *sans* filaments.